agronomy

MDPI

Article

Identification and Characterization of *Diaporthe* spp. Associated with Twig Cankers and Shoot Blight of Almonds in Spain

Maela León [1], Mónica Berbegal [1], José M. Rodríguez-Reina [2], Georgina Elena [1], Paloma Abad-Campos [1], Antonio Ramón-Albalat [1], Diego Olmo [3], Antonio Vicent [4], Jordi Luque [5], Xavier Miarnau [6], Carlos Agustí-Brisach [7], Antonio Trapero [7], Nieves Capote [8], Francisco T. Arroyo [8], Manuel Avilés [9], David Gramaje [10], Marcos Andrés-Sodupe [10] and Josep Armengol [1,*]

1 Instituto Agroforestal Mediterráneo, Universitat Politècnica de València, Camino de Vera S/N, 46022 Valencia, Spain; maela.leon@uv.es (M.L.); mobermar@etsia.upv.es (M.B.); georgina.elenajimenez@wur.nl (G.E.); pabadcam@eaf.upv.es (P.A.-C.); anraal@etsmre.upv.es (A.R.-A.)
2 Departamento de Ecosistemas Agroforestales, Universitat Politècnica de València, Camino de Vera S/N, 46022 Valencia, Spain; jorodrei@eaf.upv.es
3 Laboratori de Sanitat Vegetal, Serveis de Millora Agrària, Conselleria d'Agricultura, Medi Ambient i Territori, Govern Balear, 07009 Palma de Mallorca, Spain; dolmo@semilla-caib.es
4 Centre de Protecció Vegetal i Biotecnologia, Institut Valencià d'Investigacions Agràries (IVIA) Moncada, 46113 Valencia, Spain; avicent@ivia.es
5 Plant Pathology, Institut de Recerca i Tecnologia Agroalimentàries (IRTA), Carretera de Cabrils km 2, 08348 Cabrils, Spain; jordi.luque@irta.cat
6 Fruit Production, Institut de Recerca i Tecnologia Agroalimentàries (IRTA), Fruitcentre Building, PCiTAL, Park of Gardeny, 25003 Lleida, Spain; xavier.miarnau@irta.cat
7 Departamento de Agronomía, ETSIAM, Universidad de Córdoba, Campus de Rabanales, Edif. C4, 14071 Córdoba, Spain; cagusti@uco.es (C.A.-B.); ag1trcaa@uco.es (A.T.)
8 IFAPA Centro Las Torres, Ctra. Sevilla-Cazalla km 12,2, 41200 Alcalá del Río, Sevilla, Spain; marian.capote@juntadeandalucia.es (N.C.); franciscot.arroyo@juntadeandalucia.es (F.T.A.)
9 Departamento de Ciencias Agroforestales, Escuela Técnica Superior de Ingeniería Agronómica, Universidad de Sevilla, Ctra. Utrera km 1, 41013 Sevilla, Spain; aviles@us.es
10 Instituto de Ciencias de la Vid y del Vino (ICVV), Consejo Superior de Investigaciones Científicas–Universidad de la Rioja–Gobierno de La Rioja, Ctra. de Burgos Km. 6, 26007 Logroño, Spain; david.gramaje@icvv.es (D.G.); marcos.andres@icvv.es (M.A.-S.)
* Correspondence: jarmengo@eaf.upv.es

Received: 4 July 2020; Accepted: 22 July 2020; Published: 23 July 2020

Abstract: Two hundred and twenty-five *Diaporthe* isolates were collected from 2005 to 2019 in almond orchards showing twig cankers and shoot blight symptoms in five different regions across Spain. Multilocus DNA sequence analysis with five loci (ITS, *tub*, *tef-1α*, *cal* and *his*), allowed the identification of four known *Diaporthe* species, namely: *D. amygdali*, *D. eres*, *D. foeniculina* and *D. phaseolorum*. Moreover, a novel phylogenetic species, *D. mediterranea*, was described. *Diaporthe amygdali* was the most prevalent species, due to the largest number of isolates (85.3%) obtained from all sampled regions. The second most frequent species was *D. foeniculina* (10.2%), followed by *D. mediterranea* (3.6%), *D. eres* and *D. phaseolorum*, each with only one isolate. Pathogenicity tests were performed using one-year-old almond twigs cv. Vayro and representative isolates of the different species. Except for *D. foeniculina* and *D. phaseolorum*, all *Diaporthe* species were able to cause lesions significantly different from those developed on the uninoculated controls. *Diaporthe mediterranea* caused the most severe symptoms. These results confirm *D. amygdali* as a key pathogen of almonds in Spain. Moreover, the new species, *D. mediterranea*, should also be considered as a potential important causal agent of twig cankers and shoot blight on this crop.

Keywords: *Diaporthe amygdali*; *D. mediterranea*; multilocus DNA sequence analysis; pathogenicity; *Prunus dulcis*

1. Introduction

The worldwide cultivated area for almond (*Prunus dulcis* (Mill.) D.A. Webb) is over 2,000,000 ha. Spain, with 657,768 ha, is the country with the largest area for almond production in the world, followed by the United States, with 441,107 ha [1]. Almond is the second largest tree crop in Spain, after olive, and it is widely distributed in all regions of the country [2]. Nevertheless, Spain only contributes approximately 10% to world almond production, because the trees have been traditionally grown under rain-fed conditions and planted in marginal areas with poor soils, low rainfall and a high incidence of frost [3], thus presenting low average yields (5154 kg ha^{-1}) [1].

In recent years, almond production in Spain has been experiencing a highly favorable period, in which crop intensification, with the introduction of drip irrigation and the use of new highly productive cultivars, has increased the yield in new plantations [4]. However, the incidence of almond-associated fungal diseases, such as twig cankers and shoot blight caused by *Diaporthe* spp., is increasing and compromises crop productivity, especially in coastal areas with higher humidity and milder temperatures [5,6].

Diaporthe amygdali (Delacr.) Udayanga, Crous and K.D. Hyde is considered the causal agent of twig canker and shoot blight of almond and peach (*Prunus persica* (L.) Batsch) [7,8]. Symptoms of this disease are characterized by the quick desiccation of buds, flowers and leaves in late winter or early spring. Brown lesions (1 to 5 cm diameter), initially formed around buds on green shoots, further develop into annual sunken cankers, sometimes with a gummy exudate, as well as withering of twigs. As a result, leaves wilt and, when the disease is severe, defoliation can occur. In summer, pycnidia develop just under the dry canker epidermis [7,9,10].

The species *D. amygdali* was first described as *Fusicoccum amygdali* Delacr., associated with almond cankers in France [11]. Tuset and Portilla [9] re-examined the type specimen of *F. amygdali* and, based on morphology and symptomatology, they re-classified this fungus into *Phomopsis* as *P. amygdali* (Delacr.) J.J Tuset and M.T. Portilla. Additionally, they also considered *P. amygdalina* Canonaco to be a synonym of *P. amygdali*. Diogo et al. [8] used morphological, molecular and pathogenicity data to clarify the identity of a collection of *Phomopsis* isolates obtained from almond in Portugal. In this research, as no cultures of *P. amygdali* were linked unequivocally to any existing type, the authors proposed the fungus in voucher CBS-H 20420 (from Portugal) as the epitype for this species (isolate CBS 126679). Udayanga et al. [12] re-evaluated the phylogenetic species recognition in the genus *Diaporthe* using a multi-locus phylogeny based on the internal transcribed spacer (ITS) region of the nuclear rDNA, and partial sequences from translation elongation factor 1-α (*tef-1α*), β-tubulin (*tub*) and calmodulin (*cal*) genes. In this study, *P. amygdali* was transferred into *Diaporthe* as *D. amygdali* based on multi-locus DNA sequence data.

In recent years, the taxonomy of the genus *Diaporthe* has been deeply revised. The generic names *Diaporthe* and *Phomopsis* are no longer used to distinguish different morphs of this genus, as Rossman et al. [13] proposed that the genus name *Diaporthe* should be retained over *Phomopsis* because: (i) it was introduced before *Phomopsis* and (ii) *Diaporthe* represents the majority of species described, and therefore it has priority over *Phomopsis*. *Diaporthe* was historically considered as monophyletic based on its typical sexual morph and *Phomopsis*'s asexual morph [14]. However, Gao et al. [15] revealed its paraphyletic nature. Recent studies have demonstrated that morphological characters are inadequate to define species in this genus [16], due to their variability under changing environmental conditions [14]. Therefore, genealogical concordance methods based on multi-gene DNA sequence data provide a better approach to resolving the taxonomy for *Diaporthe* [17].

Literature about recent characterization studies of collections of *Diaporthe* isolates, obtained exclusively from almonds or including them together with isolates from other fruit or nut crops, is very scarce. Diogo et al. [8] examined *Diaporthe* isolates from almond and other *Prunus* species

in Portugal through combining morphology, pathogenicity data and a phylogenetic study based only on ITS sequences. These authors concluded that *D. amygdali* was the main species on almond, reported *D. neotheicola* for the first time on this host and a third species represented by a single isolate, which could not be unequivocally identified. Later, Lawrence et al. [18] characterized morphologically different *Diaporthe* isolates associated with wood cankers of fruit and nut crops in northern California, including three almond isolates, which were assigned to the species *D. australafricana* and *D. novem*, based on multi-gene, ITS, *tef-1α* and *cal* sequence analyses.

In Spain, the studies of Tuset and Portilla [9] and Tuset et al. [10] described almond diseases and their associated pathogens, including *D. amygdali*. These studies were based solely on the morphological characterization of the isolates. Additional studies using molecular tools to ascertain the identity of representative sets of *Diaporthe* isolates from almond in this country are lacking. Gramaje et al. [19] reported only one isolate of *D. amygdali*, which was collected from a survey of wood-associated fungal trunk pathogens of almond trees on the island of Mallorca. Thus, the objectives of the present study were: (i) to characterize a wide collection of *Diaporthe* isolates collected from almond trees in Spain by means of phenotypical characterization (fungal morphology and temperature growth) and DNA sequence analyses and (ii) to evaluate the pathogenicity of these *Diaporthe* isolates to almond twigs. The final goal was to obtain updated and more complete information about the *Diaporthe* species causing twig cankers and shoot blight of almonds in Spain.

2. Materials and Methods

2.1. Sampling and Isolation

A total of 225 *Diaporthe* isolates were collected from 2005 to 2019 in almond orchards showing twig cankers and shoot blight symptoms (Figure 1) in five different regions across Spain (Andalucía (n = 56), Islas Baleares (n = 39), Cataluña (n = 43), Comunidad Valenciana (n = 76) and La Rioja (n = 11)). Fo isolation, wood segments with cankers were cut from the affected branches, washed under running tap water, surface disinfected for 1 min in a 1.5% sodium hypochlorite solution and rinsed twice in sterile distilled water. Small pieces of affected tissues taken from the margin of the lesions were plated on potato dextrose agar (PDA; Biokar-Diagnostics, Zac de Ther, France) supplemented with 0.5 g/L of streptomycin sulphate (Sigma-Aldrich, St. Louis, MO, USA) (PDAS). Plates were incubated at 25 °C in the dark for 7 to 10 d, and all colonies were transferred to PDA. All isolates were hyphal-tipped and maintained in 15% glycerol solution at −80 °C in 1.5 mL cryovials in the fungal collection of the Instituto Agroforestal Mediterráneo–Universitat Politècnica de València (IAM-UPV) (Spain) (Table 1).

Figure 1. Twig canker and shoot blight symptoms caused by *Diaporthe* spp. on almond.

Table 1. Collection details and GenBank accession numbers of isolates included in this study.

Species	Strain Number	Year	Location	Province/Region	GenBank Accession Numbers				
					ITS	*tef-1α*	*tub*	*his*	*cal*
D. amygdali	DAL-1	2014	Sant Joan	Mallorca/Islas Baleares	MT007292	MT006769	MT006466	-	-
	DAL-2	2014	Sant Joan	Mallorca/Islas Baleares	MT007293	MT006770	MT006467	-	-
	DAL-3	2014	Santa Margalida	Mallorca/Islas Baleares	MT007294	MT006771	MT006468	MT006997	MT006694
	DAL-4	2014	Santa Margalida	Mallorca/Islas Baleares	MT007295	MT006772	MT006469	MT006998	MT006695
	DAL-5	2014	Calvià	Mallorca/Islas Baleares	MT007296	MT006773	MT006470	-	-
	DAL-7	2014	Calvià	Mallorca/Islas Baleares	MT007297	MT006774	MT006471	MT006999	-
	DAL-9	2014	Calvià	Mallorca/Islas Baleares	MT007298	MT006775	MT006472	MT007000	MT006696
	DAL-12	2014	Binissalem	Mallorca/Islas Baleares	MT007299	MT006776	MT006473	MT007001	-
	DAL-13	2014	Llucmajor	Mallorca/Islas Baleares	MT007300	MT006777	MT006474	-	-
	DAL-14	2014	Llucmajor	Mallorca/Islas Baleares	MT007301	MT006778	MT006475	-	-
	DAL-15	2014	Marratxí	Mallorca/Islas Baleares	MT007302	MT006779	MT006476	MT007002	-
	DAL-16	2014	Sa Pobla	Mallorca/Islas Baleares	MT007303	MT006780	MT006477	MT007003	MT006697
	DAL-17	2014	Sa Pobla	Mallorca/Islas Baleares	MT007304	MT006781	MT006478	-	-
	DAL-18	2014	Inca	Mallorca/Islas Baleares	MT007305	MT006782	MT006479	MT007004	-
	DAL-19	2014	Binissalem	Mallorca/Islas Baleares	MT007306	MT006783	MT006480	MT007005	-
	DAL-20	2014	Palma	Mallorca/Islas Baleares	MT007307	MT006784	MT006481	-	-
	DAL-21	2014	Binissalem	Mallorca/Islas Baleares	MT007308	MT006785	MT006482	-	-
	DAL-22	2014	Llucmajor	Mallorca/Islas Baleares	MT007309	MT006786	MT006483	MT007006	-
	DAL-23	2014	Inca	Mallorca/Islas Baleares	MT007310	MT006787	MT006484	-	-
	DAL-32	2017	Alcalalí	Alicante/Comunidad Valenciana	MT007313	MT006790	MT006487	-	-
	DAL-33	2017	Alcalalí	Alicante/Comunidad Valenciana	MT007314	MT006791	MT006488	-	-
	DAL-35	2017	Alcalalí	Alicante/Comunidad Valenciana	MT007315	MT006792	MT006489	-	-
	DAL-36	2017	Alcalalí	Alicante/Comunidad Valenciana	MT007316	MT006793	MT006490	-	-
	DAL-37	2017	Alcalalí	Alicante/Comunidad Valenciana	MT007317	MT006794	MT006491	-	-
	DAL-38	2017	Alcalalí	Alicante/Comunidad Valenciana	MT007318	MT006795	MT006492	-	-
	DAL-39	2017	Alcalalí	Alicante/Comunidad Valenciana	MT007319	MT006796	MT006493	-	-
	DAL-40	2017	Alcalalí	Alicante/Comunidad Valenciana	MT007320	MT006797	MT006494	-	-
	DAL-41	2017	Alcalalí	Alicante/Comunidad Valenciana	MT007321	MT006798	MT006495	-	-
	DAL-42	2017	Alcalalí	Alicante/Comunidad Valenciana	MT007322	MT006799	MT006496	MT007008	MT006699
	DAL-43	2017	Bunyola	Mallorca/Islas Baleares	MT007323	MT006800	MT006497	MT007009	MT006700
	DAL-44	2017	Bunyola	Mallorca/Islas Baleares	MT007324	MT006801	MT006498	-	-
	DAL-45	2017	Bunyola	Mallorca/Islas Baleares	MT007325	MT006802	MT006499	MT007010	MT006701
	DAL-46	2017	Bunyola	Mallorca/Islas Baleares	MT007326	MT006803	MT006500	-	-
	DAL-47	2017	Bunyola	Mallorca/Islas Baleares	MT007327	MT006804	MT006501	-	-
	DAL-48	2017	Bunyola	Mallorca/Islas Baleares	MT007328	MT006805	MT006502	MT007011	MT006702

Table 1. *Cont.*

Species	Strain Number	Year	Location	Province/Region	GenBank Accession Numbers				
					ITS	*tef-1α*	*tub*	*his*	*cal*
D. amygdali (cont.)	DAL-49	2017	Bunyola	Mallorca/Islas Baleares	MT007329	MT006806	MT006503	-	-
	DAL-50	2017	Bunyola	Mallorca/Islas Baleares	MT007330	MT006807	MT006504	MT007012	-
	DAL-51	2017	Bunyola	Mallorca/Islas Baleares	MT007331	MT006808	MT006505	-	-
	DAL-52	2017	Palma	Mallorca/Islas Baleares	MT007332	MT006809	MT006506	-	-
	DAL-53	2017	Palma	Mallorca/Islas Baleares	MT007333	MT006810	MT006507	-	-
	DAL-54	2017	Palma	Mallorca/Islas Baleares	MT007334	MT006811	MT006508	-	-
	DAL-55	2017	Palma	Mallorca/Islas Baleares	MT007335	MT006812	MT006509	-	-
	DAL-56	2017	Palma	Mallorca/Islas Baleares	MT007336	MT006813	MT006510	-	-
	DAL-57	2017	Palma	Mallorca/Islas Baleares	MT007337	MT006814	MT006511	MT007013	-
	DAL-65	2017	La Rinconada	Sevilla/Andalucía	MT007338	MT006815	MT006512	MT007014	-
	DAL-70	2018	Godelleta	Valencia/Comunidad Valenciana	MT007339	MT006816	MT006513	MT007015	MT006703
	DAL-71	2018	Godelleta	Valencia/Comunidad Valenciana	MT007340	MT006817	MT006514	-	-
	DAL-72	2018	Godelleta	Valencia/Comunidad Valenciana	MT007341	MT006818	MT006515	-	-
	DAL-73	2018	Godelleta	Valencia/Comunidad Valenciana	MT007342	MT006819	MT006516	-	-
	DAL-74	2018	Godelleta	Valencia/Comunidad Valenciana	MT007343	MT006820	MT006517	-	-
	DAL-75	2018	Godelleta	Valencia/Comunidad Valenciana	MT007344	MT006821	MT006518	-	-
	DAL-76	2018	Montserrat	Valencia/Comunidad Valenciana	MT007345	MT006822	MT006519	MT007016	MT006704
	DAL-77	2018	Montserrat	Valencia/Comunidad Valenciana	MT007346	MT006823	MT006520	-	-
	DAL-78	2018	Montserrat	Valencia/Comunidad Valenciana	MT007347	MT006824	MT006521	-	-
	DAL-79	2018	Montserrat	Valencia/Comunidad Valenciana	MT007348	MT006825	MT006522	-	-
	DAL-80	2018	Montserrat	Valencia/Comunidad Valenciana	MT007349	MT006826	MT006523	-	-
	DAL-81	2018	Montserrat	Valencia/Comunidad Valenciana	MT007350	MT006827	MT006524	-	-
	DAL-82	2018	Viver	Castellón/Comunidad Valenciana	MT007351	MT006828	MT006525	MT007017	MT006705
	DAL-83	2018	Viver	Castellón/Comunidad Valenciana	MT007352	MT006829	MT006526	-	-
	DAL-84	2018	Viver	Castellón/Comunidad Valenciana	MT007353	MT006830	MT006527	-	-
	DAL-85	2018	Viver	Castellón/Comunidad Valenciana	MT007354	MT006831	MT006528	MT007018	MT006706
	DAL-86	2018	Viver	Castellón/Comunidad Valenciana	MT007355	MT006832	MT006529	-	-
	DAL-87	2018	Viver	Castellón/Comunidad Valenciana	MT007356	MT006833	MT006530	-	-
	DAL-88	2018	Viver	Castellón/Comunidad Valenciana	MT007357	MT006834	MT006531	-	-
	DAL-89	2018	Viver	Castellón/Comunidad Valenciana	MT007358	MT006835	MT006532	-	-
	DAL-90	2018	Viver	Castellón/Comunidad Valenciana	MT007359	MT006836	MT006533	-	-
	DAL-91	2018	Viver	Castellón/Comunidad Valenciana	MT007360	MT006837	MT006534	-	-
	DAL-92	2018	Viver	Castellón/Comunidad Valenciana	MT007361	MT006838	MT006535	-	-
	DAL-93	2018	Viver	Castellón/Comunidad Valenciana	MT007362	MT006839	MT006536	-	-
	DAL-94	2018	Viver	Castellón/Comunidad Valenciana	MT007363	MT006840	MT006537	MT007019	-

Table 1. *Cont.*

Species	Strain Number	Year	Location	Province/Region	GenBank Accession Numbers				
					ITS	*tef-1α*	*tub*	*his*	*cal*
D. amygdali (cont.)	DAL-95	2018	Viver	Castellón/Comunidad Valenciana	MT007364	MT006841	MT006538	MT007020	-
	DAL-96	2018	Viver	Castellón/Comunidad Valenciana	MT007365	MT006842	MT006539	-	-
	DAL-97	2018	Fuente la Higuera	Valencia/Comunidad Valenciana	MT007366	MT006843	MT006540	-	-
	DAL-98	2018	Fuente la Higuera	Valencia/Comunidad Valenciana	MT007367	MT006844	MT006541	-	-
	DAL-103	2017	Gibraleón	Huelva/Andalucía	MT007368	MT006845	MT006542	MT007021	MT006707
	DAL-104	2016	El Contador	Almería/Andalucía	MT007369	MT006848	MT006543	MT007022	MT006708
	DAL-105	2017	Alcalá del Río	Sevilla/Andalucía	MT007370	MT006846	MT006544	MT007023	MT006709
	DAL-108	2018	Biar	Alicante/Comunidad Valenciana	MT007371	MT006847	MT006545	MT007024	MT006710
	DAL-109	2018	Biar	Alicante/Comunidad Valenciana	MT007372	MT006849	MT006546	-	-
	DAL-110	2018	Fuente la Higuera	Valencia/Comunidad Valenciana	MT007373	MT006850	MT006547	-	-
	DAL-111	2018	Fuente la Higuera	Valencia/Comunidad Valenciana	MT007374	MT006851	MT006548	-	-
	DAL-112	2018	Fuente la Higuera	Valencia/Comunidad Valenciana	MT007375	MT006852	MT006549	-	-
	DAL-113	2018	Fontanars dels Alforins	Valencia/Comunidad Valenciana	MT007376	MT006853	MT006550	MT007025	MT006711
	DAL-114	2018	Fontanars dels Alforins	Valencia/Comunidad Valenciana	MT007377	MT006854	MT006551	MT007026	MT006712
	DAL-116	2018	Alcublas	Valencia/Comunidad Valenciana	MT007378	MT006855	MT006552	MT007027	-
	DAL-117	2018	Alcublas	Valencia/Comunidad Valenciana	MT007379	MT006856	MT006553	-	-
	DAL-118	2018	Casinos	Valencia/Comunidad Valenciana	MT007380	MT006857	MT006554	-	-
	DAL-119	2018	Casinos	Valencia/Comunidad Valenciana	MT007381	MT006858	MT006555	-	-
	DAL-120	2018	Casinos	Valencia/Comunidad Valenciana	MT007382	MT006859	MT006556	-	-
	DAL-121	2018	Vall d'Alba	Castellón/Comunidad Valenciana	MT007383	MT006860	MT006557	MT007028	-
	DAL-122	2018	Vall d'Alba	Castellón/Comunidad Valenciana	MT007384	MT006861	MT006558	-	-
	DAL-125	2018	Vall d'Alba	Castellón/Comunidad Valenciana	MT007385	MT006862	MT006559	-	-
	DAL-126	2018	Vall d'Alba	Castellón/Comunidad Valenciana	MT007386	MT006863	MT006560	-	-
	DAL-128	2018	Godelleta	Valencia/Comunidad Valenciana	MT007387	MT006864	MT006561	-	-
	DAL-129	2018	Godelleta	Valencia/Comunidad Valenciana	MT007388	MT006865	MT006562	-	-
	DAL-130	2018	Torremendo	Alicante/Comunidad Valenciana	MT007389	MT006866	MT006563	MT007029	-
	DAL-131	2018	Torremendo	Alicante/Comunidad Valencian	MT007390	MT006867	MT006564	-	-
	DAL-132	2018	Requena	Valencia/Comunidad Valenciana	MT007391	MT006868	MT006565	MT007030	MT006713
	DAL-133	2018	Requena	Valencia/Comunidad Valenciana	MT007392	MT006869	MT006566	MT007031	-
	DAL-134	2018	Requena	Valencia/Comunidad Valenciana	MT007393	MT006870	MT006567	MT007032	-
	DAL-135	2018	L'Eliana	Valencia/Comunidad Valenciana	MT007394	MT006871	MT006568	MT007033	-
	DAL-136	2018	L'Eliana	Valencia/Comunidad Valenciana	MT007395	MT006872	MT006569	-	-
	DAL-138	2005	Constantí	Tarragona/Cataluña	MT007396	MT006873	MT006570	-	-
	DAL-139	2005	Constantí	Tarragona/Cataluña	MT007397	MT006874	MT006571	MT007034	-
	DAL-140	2012	Ulldecona	Tarragona/Cataluña	MT007398	MT006875	MT006572	MT007035	MT006714

Table 1. *Cont.*

Species	Strain Number	Year	Location	Province/Region	GenBank Accession Numbers				
					ITS	*tef-1α*	*tub*	*his*	*cal*
D. amygdali (cont.)	DAL-141	2016	Gandesa	Tarragona/Cataluña	MT007399	MT006876	MT006573	-	-
	DAL-143	2018	Gandesa	Tarragona/Cataluña	MT007400	MT006877	MT006574	-	-
	DAL-144	2018	Gandesa	Tarragona/Cataluña	MT007401	MT006878	MT006575	-	-
	DAL-145	2018	Gandesa	Tarragona/Cataluña	MT007402	MT006879	MT006576	-	-
	DAL-146	2018	Gandesa	Tarragona/Cataluña	MT007403	MT006880	MT006577	MT007036	-
	DAL-147	2018	Constantí	Tarragona/Cataluña	MT007404	MT006881	MT006578	MT007037	-
	DAL-148	2018	Constantí	Tarragona/Cataluña	MT007405	MT006882	MT006579	MT007038	-
	DAL-149	2018	Constantí	Tarragona/Cataluña	MT007406	MT006883	MT006580	MT007039	MT006715
	DAL-151	2018	Constantí	Tarragona/Cataluña	MT007407	MT006884	MT006581	-	-
	DAL-152	2018	Constantí	Tarragona/Cataluña	MT007408	MT006885	MT006582	MT007040	MT006716
	DAL-153	2018	Constantí	Tarragona/Cataluña	MT007409	MT006886	MT006583	-	-
	DAL-154	2018	La Selva del Camp	Tarragona/Cataluña	MT007410	MT006887	MT006584	MT007041	MT006717
	DAL-155	2018	La Selva del Camp	Tarragona/Cataluña	MT007411	MT006888	MT006585	MT007042	MT006718
	DAL-156	2018	La Selva del Camp	Tarragona/Cataluña	MT007412	MT006889	MT006586	-	-
	DAL-158	2018	La Selva del Camp	Tarragona/Cataluña	MT007413	MT006890	MT006587	-	-
	DAL-159	2018	La Selva del Camp	Tarragona/Cataluña	MT007414	MT006891	MT006588	-	-
	DAL-160	2018	La Selva del Camp	Tarragona/Cataluña	MT007415	MT006892	MT006589	-	-
	DAL-161	2018	Constantí	Tarragona/Cataluña	MT007416	MT006893	MT006590	-	-
	DAL-162	2018	Constantí	Tarragona/Cataluña	MT007417	MT006894	MT006591	-	-
	DAL-163	2018	Estepa	Sevilla/Andalucía	MT007418	MT006895	MT006592	-	-
	DAL-164	2018	Estepa	Sevilla/Andalucía	MT007419	MT006896	MT006593	MT007043	MT006719
	DAL-167	2018	Los Palacios	Sevilla/Andalucía	MT007420	MT006897	MT006594	MT007044	MT006720
	DAL-168	2018	Los Palacios	Sevilla/Andalucía	MT007421	MT006898	MT006595	-	-
	DAL-169	2018	Los Palacios	Sevilla/Andalucía	MT007422	MT006899	MT006596	-	-
	DAL-170	2018	Los Palacios	Sevilla/Andalucía	MT007423	MT006900	MT006597	-	-
	DAL-171	2018	Los Palacios	Sevilla/Andalucía	MT007424	MT006901	MT006598	-	-
	DAL-172	2018	Los Palacios	Sevilla/Andalucía	MT007425	MT006902	MT006599	MT007045	-
	DAL-181	2018	Córdoba	Córdoba/Andalucía	MT007426	MT006903	MT006600	MT007046	MT006721
	DAL-182	2018	Córdoba	Córdoba/Andalucía	MT007427	MT006904	MT006601	-	-
	DAL-183	2018	Córdoba	Córdoba/Andalucía	MT007428	MT006905	MT006602	-	-
	DAL-184	2018	Mairena del Alcor	Sevilla/Andalucía	MT007429	MT006906	MT006603	MT007047	-
	DAL-185	2018	Mairena del Alcor	Sevilla/Andalucía	MT007430	MT006907	MT006604	-	-
	DAL-186	2018	Mairena del Alcor	Sevilla/Andalucía	MT007431	MT006908	MT006605	-	-
	DAL-187	2018	Mairena del Alcor	Sevilla/Andalucía	MT007432	MT006909	MT006606	-	-

Table 1. *Cont.*

Species	Strain Number	Year	Location	Province/Region	GenBank Accession Numbers				
					ITS	*tef-1α*	*tub*	*his*	*cal*
D. amygdali (cont.)	DAL-188	2018	Mairena del Alcor	Sevilla/Andalucía	MT007433	MT006910	MT006607	-	-
	DAL-189	2018	Mairena del Alcor	Sevilla/Andalucía	MT007434	MT006911	MT006608	MT007048	-
	DAL-190	2018	Mairena del Alcor	Sevilla/Andalucía	MT007435	MT006912	MT006609	MT007049	MT006722
	DAL-191	2018	Mairena del Alcor	Sevilla/Andalucía	MT007436	MT006913	MT006610	-	-
	DAL-192	2018	Mairena del Alcor	Sevilla/Andalucía	MT007437	MT006914	MT006611	-	-
	DAL-193	2018	Ronda	Málaga/Andalucía	MT007438	MT006915	MT006612	MT007050	MT006723
	DAL-194	2018	Ronda	Málaga/Andalucía	MT007439	MT006916	MT006613	-	-
	DAL-195	2018	Ronda	Málaga/Andalucía	MT007440	MT006917	MT006614	-	-
	DAL-196	2018	Ronda	Málaga/Andalucía	MT007441	MT006918	MT006615	-	-
	DAL-197	2018	Ronda	Málaga/Andalucía	MT007442	MT006919	MT006616	MT007051	MT006724
	DAL-198	2018	Ronda	Málaga/Andalucía	MT007443	MT006920	MT006617	-	-
	DAL-199	2018	Ronda	Málaga/Andalucía	MT007444	MT006921	MT006618	-	-
	DAL-200	2018	Ronda	Málaga/Andalucía	MT007445	MT006922	MT006619	-	-
	DAL-201	2018	Ronda	Málaga/Andalucía	MT007446	MT006923	MT006620	-	-
	DAL-202	2018	Ronda	Málaga/Andalucía	MT007447	MT006924	MT006621	MT007052	-
	DAL-203	2018	Reus	Tarragona/Cataluña	MT007448	MT006925	MT006622	-	-
	DAL-204	2018	Reus	Tarragona/Cataluña	MT007449	MT006926	MT006623	MT007053	MT006725
	DAL-205	2018	Reus	Tarragona/Cataluña	MT007450	MT006927	MT006624	MT007054	MT006726
	DAL-206	2018	Riudoms	Tarragona/Cataluña	MT007451	MT006928	MT006625	-	-
	DAL-207	2018	Riudoms	Tarragona/Cataluña	MT007452	MT006929	MT006626	-	-
	DAL-208	2018	Riudoms	Tarragona/Cataluña	MT007453	MT006930	MT006627	MT007055	-
	DAL-209	2018	Riudoms	Tarragona/Cataluña	MT007454	MT006931	MT006628	MT007056	-
	DAL-210	2018	Riudoms	Tarragona/Cataluña	MT007455	MT006932	MT006629	MT007057	-
	DAL-211	2018	Riudoms	Tarragona/Cataluña	MT007456	MT006933	MT006630	-	-
	DAL-212	2018	Riudoms	Tarragona/Cataluña	MT007457	MT006934	MT006631	-	-
	DAL-213	2018	Riudoms	Tarragona/Cataluña	MT007458	MT006935	MT006632	-	-
	DAL-214	2018	Botarell	Tarragona/Cataluña	MT007459	MT006936	MT006633	-	-
	DAL-215	2018	Botarell	Tarragona/Cataluña	MT007460	MT006937	MT006634	MT007058	-
	DAL-216	2018	Botarell	Tarragona/Cataluña	MT007461	MT006938	MT006635	MT007059	-
	DAL-219	2018	Les Borges Blanques	Lérida/Cataluña	MT007462	MT006939	MT006636	MT007060	MT006727
	DAL-220	2018	Isona i Conca Dellà	Lérida/Cataluña	MT007463	MT006940	MT006637	MT007061	MT006728
	DAL-221	2018	Isona i Conca Dellà	Lérida/Cataluña	MT007464	MT006941	MT006638	MT007062	-
	DAL-225	2019	Murillo	Logroño/La Rioja	MT007465	MT006942	MT006639	MT007063	MT006729
	DAL-226	2019	Murillo	Logroño/La Rioja	MT007466	MT006943	MT006640	-	-

Table 1. *Cont.*

Species	Strain Number	Year	Location	Province/Region	GenBank Accession Numbers				
					ITS	*tef-1α*	*tub*	*his*	*cal*
D. amygdali (cont.)	DAL-227	2019	Santa Engracia de Jubera	Logroño/La Rioja	MT007467	MT006944	MT006641	MT007064	MT006730
	DAL-228	2019	Santa Engracia de Jubera	Logroño/La Rioja	MT007468	MT006945	MT006642	-	-
	DAL-229	2019	Santa Engracia de Jubera	Logroño/La Rioja	MT007469	MT006946	MT006643	-	-
	DAL-230	2019	Santa Engracia de Jubera	Logroño/La Rioja	MT007470	MT006947	MT006644	-	-
	DAL-231	2019	Santa Engracia de Jubera	Logroño/La Rioja	MT007471	MT006948	MT006645	-	-
	DAL-232	2019	Santa Engracia de Jubera	Logroño/La Rioja	MT007472	MT006949	MT006646	-	-
	DAL-233	2019	Lagunilla	Logroño/La Rioja	MT007473	MT006950	MT006647	MT007065	MT006731
	DAL-234	2019	Santa Engracia de Jubera	Logroño/La Rioja	MT007474	MT006951	MT006648	-	-
	DAL-236	2019	Alcalá del Río	Sevilla/Andalucía	MT007475	MT006952	MT006649	MT007066	-
	DAL-237	2019	Alcalá del Río	Sevilla/Andalucía	MT007476	MT006953	MT006650	-	-
	DAL-238	2019	Alcalá del Río	Sevilla/Andalucía	MT007477	MT006954	MT006651	-	-
	DAL-239	2019	Córdoba	Córdoba/Andalucía	MT007478	MT006955	MT006652	-	-
	DAL-240	2019	Córdoba	Córdoba/Andalucía	MT007479	MT006956	MT006653	MT007067	MT006732
	DAL-241	2019	Córdoba	Córdoba/Andalucía	MT007480	MT006957	MT006654	-	-
	DAL-242	2019	Santa Cruz	Córdoba/Andalucía	MT007481	MT006958	MT006655	-	-
	DAL-243	2019	Córdoba	Córdoba/Andalucía	MT007482	MT006959	MT006656	-	-
	DAL-244	2019	Villamanrique de la Condesa	Sevilla/Andalucía	MT007483	MT006960	MT006657	MT007068	MT006733
	DAL-245	2019	Villamanrique de la Condesa	Sevilla/Andalucía	MT007484	MT006961	MT006658	-	-
	DAL-246	2019	Santa Engracia de Jubera	Logroño/La Rioja	MT007485	MT006962	MT006659	-	-
D. eres	DAL-102	2016	Córdoba	Córdoba/Andalucía	MN997106	MT007104	MT006462	MT007106	MT006465
D. foeniculina	DAL-10	2014	Santa Margalida i Calvià	Mallorca/Islas Baleares	MT007497	MT006963	MT006660	MT007069	MT006734
	DAL-11	2014		Mallorca/Islas Baleares	MT007498	MT006964	MT006661	MT007070	MT006735
	DAL-27	2017	Alcalalí	Alicante/Comunidad Valenciana	MT007499	MT006965	MT006662	MT007071	MT006736
	DAL-28	2017	Alcalalí	Alicante/Comunidad Valenciana	MT007500	MT006966	MT006663	MT007072	MT006737
	DAL-30	2017	Alcalalí	Alicante/Comunidad Valenciana	MT007501	MT006967	MT006664	MT007073	MT006738
	DAL-31	2017	Alcalalí	Alicante/Comunidad Valenciana	MT007502	MT006968	MT006665	MT007074	MT006739
	DAL-61	2016	Alcalá del Río	Sevilla/Andalucía	MT007503	MT006969	MT006666	MT007075	MT006740
	DAL-62	2016	Alcalá del Río	Sevilla/Andalucía	MT007504	MT006970	MT006667	MT007076	MT006741
	DAL-63	2016	Alcalá del Río	Sevilla/Andalucía	MT007505	MT006971	MT006668	MT007077	MT006742
	DAL-64	2016	Alcalá del Río	Sevilla/Andalucía	MT007506	MT006972	MT006669	MT007078	MT006743
	DAL-66	2017	La Rinconada	Sevilla/Andalucía	MT007507	MT006973	MT006670	MT007079	MT006744
	DAL-67	2017	La Rinconada	Sevilla/Andalucía	MT007508	MT006974	MT006671	MT007080	MT006745
	DAL-68	2017	La Rinconada	Sevilla/Andalucía	MT007509	MT006975	MT006672	MT007081	MT006746
	DAL-69	2017	La Rinconada	Sevilla/Andalucía	MT007510	MT006976	MT006673	MT007082	MT006747
	DAL-99	2018	Fuente la Higuera	Valencia/Comunidad Valenciana	MT007511	MT006977	MT006674	MT007083	MT006748
	DAL-100	2018	Fuente la Higuera	Valencia/Comunidad Valenciana	MT007512	MT006978	MT006675	MT007084	MT006749

Table 1. *Cont.*

Species	Strain Number	Year	Location	Province/Region	GenBank Accession Numbers				
					ITS	*tef-1α*	*tub*	*his*	*cal*
D. foeniculina (cont.)	DAL-101	2018	Fuente la Higuera	Valencia/Comunidad Valenciana	MT007513	MT006979	MT006676	MT007085	MT006750
	DAL-107	2018	Marchena	Sevilla/Andalucía	MT007514	MT006980	MT006677	MT007086	MT006751
	DAL-142	2018	Cabrils	Barcelona/Cataluña	MT007515	MT006981	MT006678	MT007087	MT006752
	DAL-150	2018	Constantí	Tarragona/Cataluña	MT007516	MT006982	MT006679	MT007088	MT006753
	DAL-157	2018	La Selva del Camp	Tarragona/Cataluña	MT007517	MT006983	MT006680	MT007089	MT006754
	DAL-165	2018	Estepa	Sevilla/Andalucía	MT007518	MT006984	MT006681	MT007090	MT006755
	DAL-217	2018	Les Borges Blanques	Lérida/Cataluña	MT007519	MT006985	MT006682	MT007091	MT006756
D. mediterranea	DAL-6	2014	Calvià	Mallorca/Islas Baleares	MT007486	MT006986	MT006683	MT007092	MT006758
	DAL-8	2014	Consell	Mallorca/Islas Baleares	MT007487	MT006987	MT006684	MT007093	MT006759
	DAL-24	2014	Sant Llorenç d'Escardassar	Mallorca/Islas Baleares	MT007488	MT006988	MT006685	MT007094	MT006760
	DAL-34	2017	Alcalalí	Alicante/Comunidad Valenciana	MT007489	MT006989	MT006686	MT007095	MT006761
	DAL-173	2018	Altea la Vella	Alicante/Comunidad Valenciana	MT007493	MT006993	MT006691	MT007099	MT006765
	DAL-174	2018	Altea la Vella	Alicante/Comunidad Valenciana	MT007494	MT006994	MT006690	MT007100	MT006766
	DAL-175	2018	Altea la Vella	Alicante/Comunidad Valenciana	MT007495	MT006995	MT006692	MT007101	MT006767
	DAL-176	2018	Altea la Vella	Alicante/Comunidad Valenciana	MT007496	MT006996	MT006693	MT007102	MT006768
D. phaseolorum	DAL-222	2016	Alcalá del Río	Sevilla/Andalucía	MN997107	MT007103	MT006463	MT007105	MT006464

2.2. DNA Extraction, PCR Amplification and Sequencing

Mycelium was scraped from 10-day-old fungal cultures grown on PDA medium. Total fungal DNA was extracted using the E.Z.N.A. Plant DNA Kit (Omega Bio-tek, Norcross, GA, USA), following the manufacturer's short protocol instructions.

The ITS region and fragments of *tub* and *tef-1α* genes were amplified and sequenced. Based on these preliminary results, representative isolates were selected for amplifying and sequencing *cal* and histone H3 (*his*) genes. Amplification by polymerase chain reaction (PCR) was performed in a total volume of 25 µL using HotBegan™ Taq DNA Polymerase (Canvax Biotech SL, Córdoba, Spain), according to the manufacturer's instructions on a Peltier Thermal Cycler-200 (MJ Research). One reaction was composed of 2.5 µL of 10× PCR Buffer B, 2.5 µL of MgCl2 (25 mM), 2.5 µL of dNTPs (8 mM), 1 µL of each primer (10 µM), 0.2 µL of HotBegan Taq DNA Polymerase (5 U/µL), 1 µL of purified template DNA and 14.3 µL of nuclease-free water. The thermal cycle consisted of an initial step of 3 min at 94 °C, followed by 35 cycles of denaturation at 94 °C for 30 s, annealing for 30 s and elongation at 72 °C for 45 s. A final extension was performed at 72 °C for 5 min. The primers pairs and the annealing temperatures (Ta) for each locus were as follows: ITS1-F and ITS4 for ITS (Ta = 55 °C) [20,21], EF1-688F and EF1-1251R for *tef-1α* (Ta = 55 °C) [22], BtCadF and BtCadR or T1 and BT2b for *tub* (Ta = 55 °C for both pairs) [23–25], CYLH3F and H3-1b for *his* (Ta = 58 °C) [25,26], CL1C and CL2C or CAL-563F and CL2C for *cal* (Ta = 58 °C for both pairs) [27,28]. PCR products were analyzed by 1% agarose gel electrophoresis, purified and sequenced by Macrogen Inc. (Madrid, Spain) using both PCR primers. Each consensus sequence was assembled using Sequencher software 5.0 (Gene Codes Corp., Ann Arbor, Michigan).

2.3. Phylogenetic Analyses

Sequences generated in this study were compared with reference sequences in the GenBank nucleotide database to determine the closest relatives for the phylogenetic studies. Fo each of the five loci (ITS, *tub*, *tef-1α*, *cal* and *his*), the DNA sequences obtained in this study (Table 1), together with those retrieved from GenBank (Table 2), were aligned using the ClustalW algorithm included in the MEGAX software package [29,30]. The alignments were analyzed and adjusted manually when necessary. Ambiguous sequences at either end of the alignments were excluded prior to analyses. Concatenated datasets were built in Sequence Matrix v.1.8 [31].

Table 2. Additional *Diaporthe* species used in the phylogenetic analyses.

Species	Strain	Host	Country	GenBank Accession Numbers				
				ITS	*tef-1α*	*tub*	*his*	*cal*
D. acaciigena	**CBS 129521**	*Acacia retinodes*	Australia	KC343005	KC343731	KC343973	KC343489	KC343247
D. amygdali	**CBS 126679**	*Prunus dulcis*	Portugal	KC343022	KC343748	KC343990	KC343506	KC343264
	CBS 111811	*Vitis vinifera*	South Africa	KC343019	KC343745	KC343987	KC343503	KC343261
D. celastrina	**CBS 139.27**	*Celastrus scandens*	USA	KC343047	KC343773	KC344015	KC343531	KC343289
D. celeris	**CBS 143349**	*Vitis vinifera*	UK	MG281017	MG281538	MG281190	MG281363	MG281712
	CBS 143350	*Vitis vinifera*	UK	MG281018	MG281539	MG281191	MG281364	MG281713
D. chamaeropis	CBS 454.81	*Chamaerops humilis*	Greece	KC343048	KC343774	KC344016	KC343532	KC343290
	CBS 753.70	*Spartium junceum*	Croatia	KC343049	KC343775	KC344017	KC343533	KC343291
D. chongqingensis	**PSCG 435**	*Pyrus pyrifolia*	China	MK626916	MK654866	MK691321	MK726257	MK691209
	PSCG 436	*Pyrus pyrifolia*	China	MK626917	MK654867	MK691322	MK726256	MK691208
D. cinerascens	CBS 719.96	*Ficus carica*	Bulgaria	KC343050	KC343776	KC344018	KC343534	KC343292
D. endophytica	**CBS 133811**	*Schinus terebinthifolius*	Brazil	KC343065	KC343791	KC344033	KC343549	KC343307
	LGMF911	*Schinus terebinthifolius*	Brazil	KC343066	KC343792	KC344034	KC343550	KC343308
D. eres	**CBS 138594**	*Ulmus laevis*	Germany	KJ210529	KJ210550	KJ420799	KJ420850	KJ434999
	CBS 109767	*Acer campestre*	Austria	KC343075	KC343801	KC344043	KC343559	KC343317
D. foeniculina	**CBS 111553**	*Foeniculum vulgare*	Spain	KC343101	KC343827	KC344069	KC343585	KC343343
	CBS 187.27	*Camellia sinensis*	Italy	KC343107	KC343833	KC344075	KC343591	KC343349
D. fusicola	**CGMCC 3.17087**	*Lithocarpus glabra*	China	KF576281	KF576256	KF576305	-	KF576233
	CGMCC 3.17088	*Lithocarpus glabra*	China	KF576263	KF576238	KF576287	-	KF576221
D. garethjonesii	**MFLUCC 12-0542A**	Unknown dead leaf	Thailand	KT459423	KT459457	KT459441	-	KT459470
D. helicis	CBS 138596	*Hederahelix*	Germany	KJ210538	KJ210559	KJ420828	KJ420875	KJ435043
D. kadsurae	**CFCC 52586**	*Kadsura longipedunculata*	China	MH121521	MH121563	MH121600	MH121479	MH121439
	CFCC 52587	*Kadsura longipedunculata*	China	MH121522	MH121564	MH121601	MH121480	MH121440
D. masirevicii	BRIP 54120c	*Zea mays*	Australia	KJ197278	KJ197240	KJ197258	-	-
	BRIP 57892a	*Helianthus annuus*	Australia	KJ197276	KJ197239	KJ197257	-	-
D. ovalispora	ICMP20659	*Citrus limon*	China	KJ490628	KJ490507	KJ490449	KJ490570	-
D. ovoicicola	CGMCC 3.17092	*Lithocarpus glabra*	China	KF576264	KF576239	KF576288	-	KF576222
	CGMCC 3.17093	*Citrus* sp.	China	KF576265	KF576240	KF576289	-	KF576223
D. phaseolorum	CBS 113425	*Olearia* cf. *rani*	New Zealand	KC343174	KC343900	KC344142	KC343658	KC343416
	CBS 116019	*Caperonia palustris*	USA	KC343175	KC343901	KC344143	KC343659	KC343417
D. pulla	**CBS 338.89**	*Hedera helix*	Croatia	KC343152	KC343878	KC344120	KC343636	KC343394
D. pustulata	CBS 109742	*Acer pseudoplatanus*	Austria	KC343185	KC343911	KC344153	KC343669	KC343427
	CBS 109784	*Prunus padus*	Austria	KC343187	KC343913	KC344155	KC343671	KC343429

Table 2. *Cont.*

Species	Strain	Host	Country	GenBank Accession Numbers				
				ITS	*tef-1α*	*tub*	*his*	*cal*
D. sojae	CBS 100.87	*Glycine soja*	Italy	KC343196	KC343922	KC344164	KC343680	KC343438
	CBS 116017	*Euphorbia nutans*	USA	KC343197	KC343923	KC344165	KC343681	KC343439
D. sterilis	**CBS 136969**	*Vaccinium corymbosum*	Italy	KJ160579	KJ160611	KJ160528	MF418350	KJ160548
	CBS 136970	*Vaccinium corymbosum*	Italy	KJ160580	KJ160612	KJ160529	-	KJ160549
D. subellipicola	MFLUCC 17-1197	On dead wood	China	MG746632	MG746633	MG746634	-	-
Diaporthella corylina	CBS 121124	*Corylus* sp.	China	KC343004	KC343730	KC343972	KC343488	KC343246
Phomopsis sp. 5	PMM1657	*Vitis vinifera*	South Africa	KY511331	-	KY511363	-	-
	PMM1660	*Vitis vinifera*	South Africa	KY511333	-	KY511365	-	-

Note. **BRIP**: Queensland Plant Pathology Herbarium, Brisbane, Queensland, Australia; **CBS**: Westerdijk Fungal Biodiversity Institute, Utrecht, The Netherlands; **CFCC**: China Forestry Culture Collection Center; **CGMCC**: China General Microbiological Culture Collection, Beijing, China; **ICMP**: International Collection of Microorganisms from Plants, Auckland, New Zealand; **LGMF**: Culture collection of the Laboratory of Genetics of Microorganisms, Federal University of Parana, Curitiba, Brazil; **MFLUCC**: Mae Fah Luang University Culture Collection, Chiang Rai, Thailand; **PMM**: Lesuthu et al., 2019. Ex-type isolates are indicated in bold.

Phylogenetic analyses were based on Bayesian inference (BI), maximum likelihood (ML) and maximum parsimony (MP). Bayesian analyses were performed using MrBayes v 3.2 on the CIPRES Science Gateway v 3.3 [32,33]. The best-fitting model of nucleotide evolution for each partition was determined by MrModeltest 2.3 using the Akaike information criterion (AIC) [34]. Four simultaneous analyses were run for 100 million generations, sampling every 10,000, with four Markov chain Monte Carlo (MCMC) chains. The first 25% of saved trees were discarded and posterior probabilities were determined from the remaining trees. The ML analyses were done with the tool Randomized Axelerated Maximum Likelihood RAxML-HPC2 on XSEDE implemented on CIPRES Science Gateway v 3.3 [35]. ML tree searches were performed under the generalized time-reversible with gamma correction (GTR + Γ) nucleotide substitution model using 1000 pseudoreplicates. The other parameters were used as default settings. MP analyses were performed in MEGA X with the tree Bisection and reconnection (TBR) algorithm, where gaps were treated as missing data. The robustness of the topology was evaluated by 1000 bootstrap replications [36]. Measures for the maximum parsimony as tree length (TL), consistency index (CI), retention index (RI) and rescaled consistency index (RC) were also calculated.

New sequences obtained in this study were deposited in GenBank (Table 1) and the multilocus alignment in was deposited in TreeBASE (http://purl.org/phylo/treebase/phylows/study/TB2:S26453).

2.4. Taxonomy

Agar plugs (6-mm diameter) were taken from the edge of actively growing cultures on PDA and transferred onto the center of 9-cm diameter Petri dishes containing one of the following culture media: malt extract agar (MEA; Sigma-Aldrich Laboratories), PDA, 2% tap water agar supplemented with sterile pine needles (PNA) or and oatmeal agar (OA; 60 g oatmeal, 12.5 g agar, Difco, Le Pont de Claix, France). Plates were then incubated at 21–22 °C under a 12 h/12 h near-ultraviolet light/darkness cycle to induce sporulation as described by Guarnaccia et al. (2018). Cultures were examined periodically for the development of ascomata and conidiomata. Colony colors were rated only on PDA after 15 days of incubation according to Rayner [37]. Morphological characteristics were examined using an Axio Scope A.1 microscope (Zeiss, manufacturer data) after mounting single pycnidia in lactic acid. Fungal structures were measured (30 measurements per type of structure) using the Zeiss AxioVision LE imaging device. Photos were captured using a Zeiss AxioCam MRm digital camera from images recorded with the 40× objective. Descriptions, nomenclature and illustrations of taxonomic novelties were deposited in MycoBank (MB 836048).

The effect of temperature on the mycelial growth of selected isolates of the species *D. mediterranea* (DAL24, DAL34 and DAL174) was measured on PDA. Fo this purpose, agar plugs (6-mm diameter) obtained from the growing edge of colonies were transferred to the center of PDA plates, which were incubated at 5, 10, 15, 20, 25, 30, 35 or 40 °C in darkness. Four replicates for each isolate and temperature combination were used. Growth was determined after 7 days in two orthogonal directions, and the mean growth rate was calculated in mm/day using a simplified version of the non-linear equation proposed by Duthie et al. [38]. Regression curves were fitted to the data using the R function "nls" included in the "stats" package [39,40].

2.5. Pathogenicity Tests

Pathogenicity tests were conducted as described by Diogo et al. [8]. One-year-old twigs of almond cv. Vayro, about 30 cm long, were inoculated with a set of 14 representative isolates of the five *Diaporthe* species found associated with *P. dulcis* in this study: *D. amydgali* (isolates DAL-3, DAL-4, DAL-45, DAL-70, DAL-105, DAL-140 and DAL-159), *D. eres* (DAL-102), *D. foeniculina* (DAL-27 and DAL-61), *D. phaseolorum* (DAL-222) and *D. mediterranea* (DAL-24, DAL-34 and DAL-174). These isolates were selected to represent diverse geographical origins. The twigs were surface sterilized by immersion in 70% ethanol for 30 s, 1.5% sodium hypochlorite solution for 1 min and ethanol for 30 s. Then, they were air dried in a laminar flow cabinet.

Wounds were made in the center of each twig with a 6-mm cork borer. Colonized agar plugs with mycelium of about the same size, which were obtained from active 10-day-old colonies growing on PDA, were inserted underneath the epidermis and the wounds were sealed with Parafilm. Inoculated twigs were kept in an upright position with their lower ends immersed in 1 L jars with 500 mL of sterile water in a growth chamber at 23 °C with 12 h of light per day. The twigs were covered with a plastic bag during the first 4 days to keep a moist environment. Six twigs per isolate were used and a negative control was prepared using uncolonized PDA plugs. Jars were arranged in a completely randomized design and the water was changed every 3 days. The experiment was repeated once.

Lesion lengths were measured 15 days after inoculation. Immediately after lesion measurements, two representative shoots per inoculated isolate and replicate were surface sterilized as described above. Small internal fragments were cut from the margin of the healthy and necrotic tissue and placed onto PDA. Plates were incubated at 25 °C in the dark for 7 to 10 d, and all fungal growths resembling *Diaporthe* were transferred to PDA. A representative subsample, one culture from each of the 14 isolates and replicates, were subjected to DNA extraction and molecular identification as described above to satisfy Koch's postulates.

Significance levels for mean values of lesion length (cm), corresponding to different *Diaporthe* spp. isolates inoculated and control detached twigs, were determined. The analyses were performed considering individual isolates and groups of isolates from each *Diaporthe* spp. ANOVA assumptions were verified using Shapiro–Wilk and Levene's tests. The datasets did not meet ANOVA assumptions, thus the analysis was performed using the Kruskal–Wallis test. Control twigs were compared with the inoculated ones considering individual isolates, and different species were compared with *D. amygdali* using the Wilcoxon rank sum test ($p < 0.01$). The analyses were performed in R using the agricolae and stats packages [39,40].

3. Results

3.1. Phylogenetic Analyses

Three loci (ITS region and fragments of *tub* and *tef-1α* genes) were sequenced in all *Diaporthe* isolates (n = 225) obtained in this study and compared with those in GenBank. The BLAST search showed high identity with *D. amygdali*, *D. eres*, *D. foeniculina* and *D. phaseolorum* accessions. Fo phylogenetic analyses, two representative isolates of closely related species, i.e., the ex-type together with one additional isolate when possible, were selected as references, and their corresponding sequences were retrieved from GenBank (Table 2). These sequences (n = 38), including *Diaporthella corylina* strain CBS 121124 which was used as outgroup, were added to those of the Spanish isolates (n = 225). The MP three-locus phylogeny showed that Spanish isolates of *Diaporthe* grouped into five distinct clades, four of them with known *Diaporthe* species (data not shown). The most abundant group, with 192 isolates, clustered with the ex-type isolate of *D. amygdali* (CBS 126679), the second (n = 23) with the ex-type of *D. foeniculina* (CBS 111553) and two single isolates each grouped with the ex-type of *D. eres* (CBS 109767), and with *D. phaseolorum* (CBS 116019). The remaining isolates (n = 8) clustered together, closely related to, but separated from, *D. sterilis* (CBS136969), suggesting that they could belong to a new species.

For accurate resolution of the species limits of our isolates, fragments of *his* and *cal* genes were sequenced in a set of 70 and 39 representative *D. amygdali* isolates, respectively, and for all isolates of the other groups (Table 1). The selection of the *D. amygdali* isolates was based on the province/region of origin and year of isolation. In addition, all GenBank sequences (ITS and *tub*) of two undescribed *Diaporthe* isolates (PMM 1657 and PMM 1660), which shared 100% identity with these loci of the potential new species, were included in the analyses (Table 2). Then, MP, ML and BI phylogenetic trees were constructed for the five-locus combined dataset, which included all taxa (n = 265) regardless of the level of completeness. A total of 2826 characters, including gaps (ITS: 1–564, *tub*: 565–1384, *tef-1α*: 1385–1814, *his*: 1815–2300 and *cal*: 2301–2826), were used in phylogenetic analyses, of which 1494 were

constant and 817 were parsimony informative. The MP analysis yielded a single most parsimonious tree (TL = 2387; CI = 0.647; RI = 0.955; RC = 0.618). The ML analysis resulted in a single best tree with the final ML optimization likelihood = −15029.27737. In the BI analysis, the ITS/*tub*/*tef-1α*/*his*/*cal* partitions had 158/341/310/210/308 unique site patterns, respectively, and the analysis read a total of 40,004 trees, sampling 30,004 of them. The topologies and branching order of the inferred trees were compared visually, and they were fully congruent among themselves and with the previous ITS/*tub*/*tef-1α* multilocus phylogeny. The ITS/*tub*/*tef-1α*/*his*/*cal* ML tree is presented with the support of all phylogenetic methods at the branches (Figure 2).

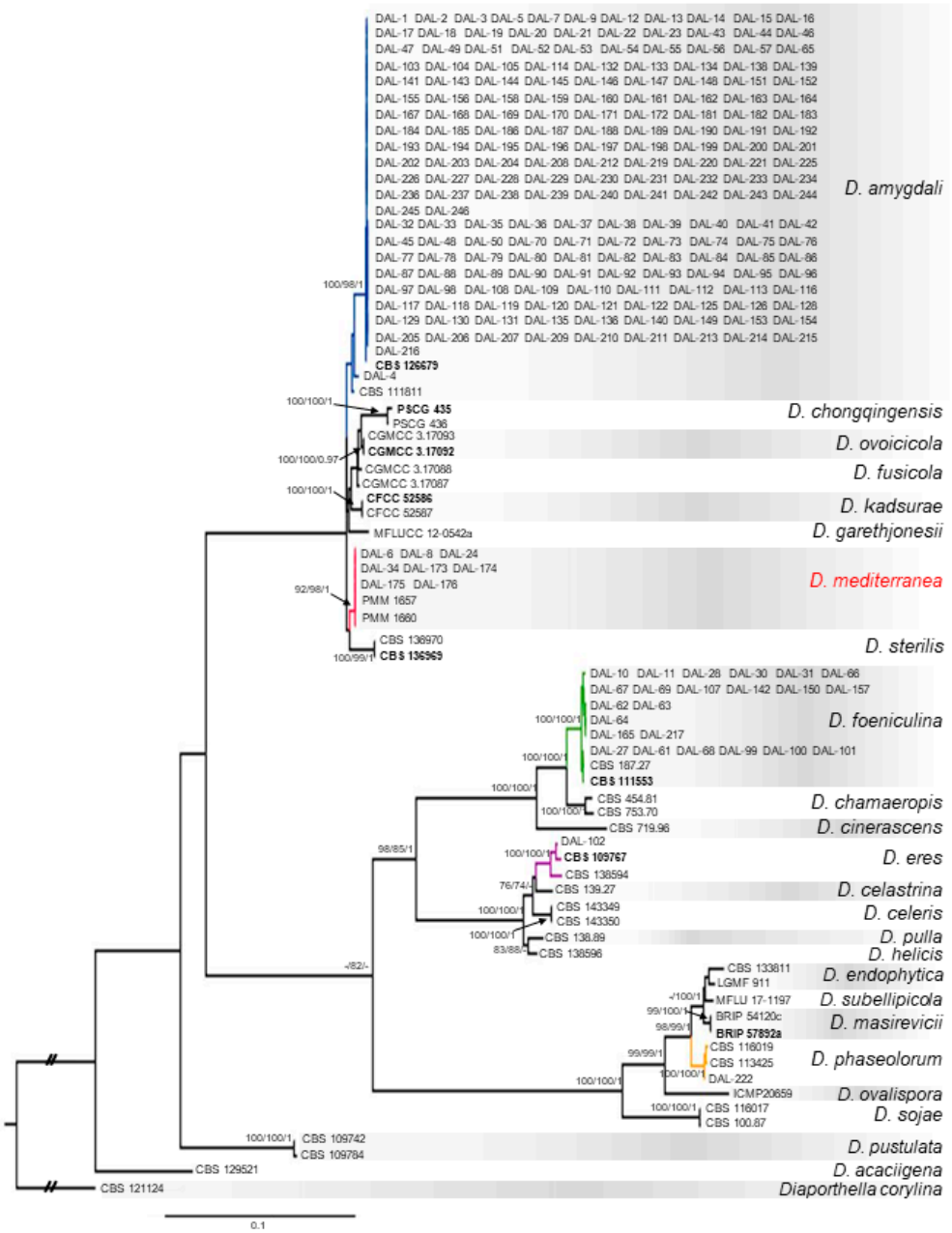

Figure 2. Randomized Axelerated Maximum Likelihood (RAxML) tree based on analysis of a combined dataset of ITS, *tub*, *tef-1α*, *his* and *cal* sequences. Bootstrap support values for Maximum Parsimony (MP) and ML higher than 70% and Bayesian posterior probabilities (PP) higher than 0.90 are shown at the branches (MP/ML/PP). Clades highlighted contain the isolates identified in the current study and the novel taxa is shown in red. Ex-type strains are indicated in bold. The tree is rooted using *Diaporthella corylina* (CBS121124). The scale bar represents the expected number of nucleotide substitutions per site.

Diaporthe amygdali represented 85.3% of the studied isolates and they were obtained from all sampled regions. The second most frequent species was *D. foeniculina*, with 23 isolates (10.2% of total), and it was recovered in all sampled regions except in La Rioja. *Diaporthe eres* and *D. phaseolorum*, each with only one isolate, were recovered from the Andalucía region. The remaining isolates (n = 8, 3.6% of total) were grouped together with 92% and 98% bootstrap support for MP and ML, respectively, and with 1 of BI posterior probability, but not with any known *Diaporthe* species. Therefore, they were putatively identified as belonging to a novel species described here and named *D. mediterranea*. This new species was obtained from the Islas Baleares and Comunidad Valenciana regions.

3.2. Taxonomy

Based on both the results of the phylogenetic inference and morphological characters, one new species of *Diaporthe* is described below (Figure 3).

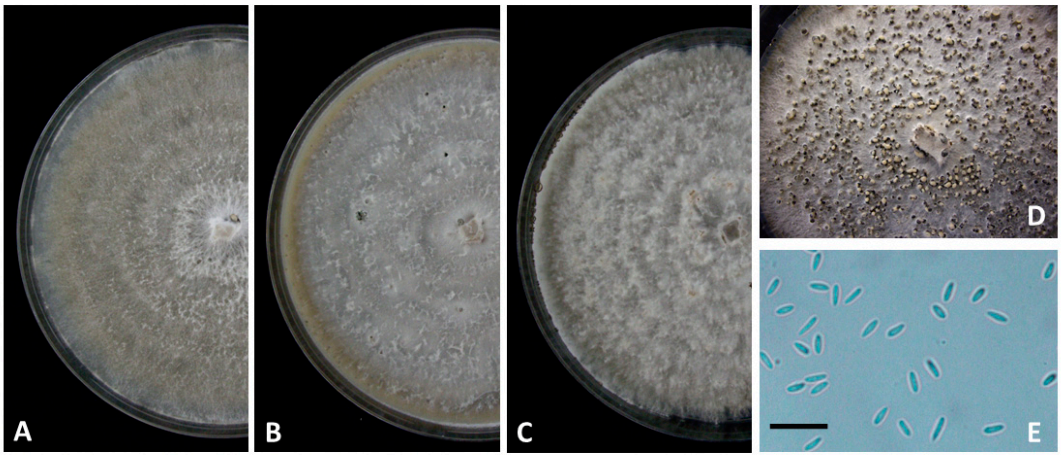

Figure 3. *Diaporthe mediterranea* (DAL-34). (**A**–**C**) Colonies on Malt Extract Agar (MEA), Oat Agar (OA) and Potato Dextrose Agar (PDA), respectively; (**D**) conidiomata sporulating on PDA; (**E**) alpha conidia—scale bar = 20 µm.

Diaporthe mediterranea M. León, J. M. Rodríguez-Reina and J. Armengol, **sp. nov.**—MycoBank MB 836048; Figure 3.

Typification: Alcalalí, Alicante province (Comunidad Valenciana), Spain. From *Prunus dulcis* twig canker, 2017, J. Armengol, DAL-34 (holotype; CBS H-24368—ex-type culture CBS 146754).

Etymology. Named after the Mediterranean Sea, because this species was found on almond trees from orchards located in the Alicante province (Comunidad Valenciana) and Mallorca (Islas Baleares) in Mediterranean coastal areas of Spain.

Known distribution: Spain.

Description: Conidiomata pycnidial, globose or irregular, solitary on PNA but also aggregated on MEA, PDA and OA, erumpent, dark brown to black, (mean diameter ± SD = 527 ± 104.8 µm, n = 30), whitish translucent to creamy conidial drops exuded from the ostioles. Conidiophores densely aggregated lining the inner cavity, smooth and hyaline, cylindrical, straight, reduced to conidiogenous cells (mean ± SD =15.5 ± 2.7 × 2.2 ± 0.4 µm, n = 30). Paraphyses not observed. Alpha conidia produced in all the tested media, aseptate, fusiform, hyaline, multi-guttulate and acute at both ends, (mean ± SD = 6.6 ± 0.5 × 2.4 ± 0.2 µm, n = 30). Beta and gamma conidia not observed.

Culture characteristics: Colonies covering the medium within 7 d at 25 °C, with moderate aerial mycelium. Colonies on MEA, PDA and OA white at first, becoming light cream, mycelium flat on MEA and OA, denser and more felted on PDA. Reverse pale brown with light to dark grayish dots with age, with visible solitary and aggregate conidiomata at maturity on MEA, PDA and OA. Optimum growth temperature on PDA was 25.4 °C. Growth rates of colonies on PDA at 5, 10, 15, 20, 25, 30 and

35 °C were 0.02, 0.11, 0.36, 0.44, 0.67, 0.57 and 0.01 mm per day, respectively. No growth was observed at 40 °C.

Additional materials examined: DAL24 Sant Llorenç d'Escardassar, Mallorca, Islas Baleares, Spain, 2014 and DAL174 Altea la Vella, Alicante, Comunidad Valenciana, Spain, 2018.

Notes: *Diaporthe mediterranea* was collected from *P. dulcis* in Spain. The BLASTn search showed 100% identity with the available sequences (ITS and *tub*) of two isolates named *Phomopsis* sp. 5 (PMM 1657 and PMM 1660), collected from *Vitis vinifera* in South Africa [41,42], which were not described as new species by any of the authors. Nevertheless, other loci are needed to better resolve the identity of these isolates. Phylogenetic analysis combining five gene loci showed that all the isolates of *D. mediterranea* clustered together in a highly supported clade (92/98/1) and displayed a close relationship but they were clearly differentiated from *D. sterilis.* Based on alignments of the separate loci, *D. mediterranea* differs from *D. sterilis* [43] in seven positions (6 nt and one indel of 1 nt) of 426 bp in *tub* (p-distance = 1.4%), 20 positions (4 nt and one indel of 16 nt) of 342 bp in *tef1-α* (p-distance = 1.5%), 21 nt of 434 bp in *his* (p-distance = 4.8%), and 3 nt of 469 bp in *cal* (p-distance = 0.6%). The ITS sequences of both species showed 100% identity. Morphologically, *D. mediterranea* mainly differs from *D. sterilis* in its capacity to produce alpha conidia, because all isolates representing *D. sterilis* could not be induced to sporulate on any of the culture media used by Lombard et al. [43], when this new *Diaporthe* species collected from *Vaccinium corymbosum* was described.

3.3. Pathogenicity Tests

All *Diaporthe* isolates inoculated on one-year-old twigs of almond cv. Vayro caused necrotic lesions of variable length (Figure 4). There was no effect of the experiment on the lesion length ($p = 0.5032$). Mean lesion length in canes inoculated with different *Diaporthe* isolates (n = 12 per inoculated isolate) ranged from 1.4 to 13.7 cm and control twigs treated with uncolonized PDA plugs showed a mean lesion length of 0.6 cm (Figure 5). Statistical analysis revealed significant differences in lesion length between the control and twigs inoculated with all isolates, except those of *D. foeniculina*, namely DAL-27 and DAL-61 ($p = 0.7224$ and $p = 0.0117$, respectively) and *D. phaseolorum* DAL-222 ($p = 0.0239$).

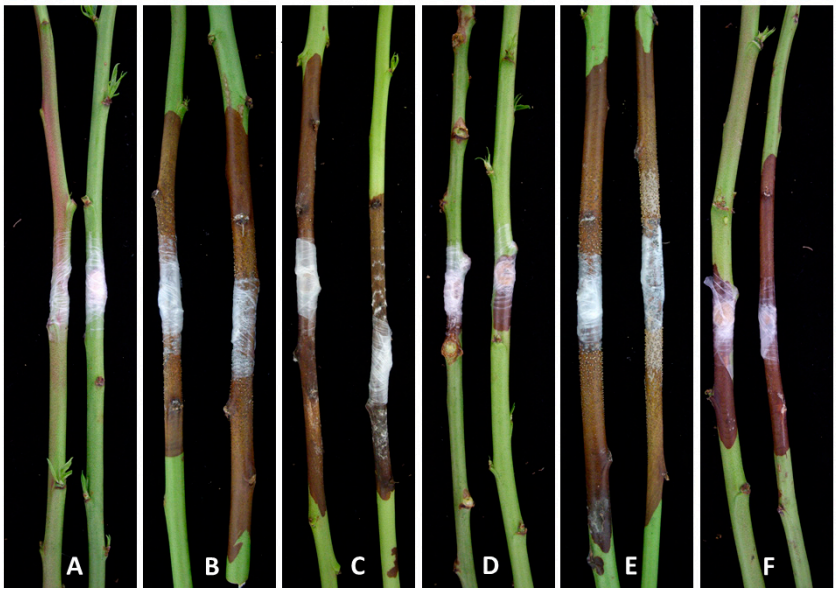

Figure 4. Necrotic lesions induced by the *Diaporthe* spp. inoculated on almond detached canes. (**A**) Uninoculated control; (**B**) *D. amygdali* (DAL-4); (**C**) *D. eres* (DAL-102); (**D**) *D. foeniculina* (DAL-61); (**E**) *D. mediterranea* (DAL-34) and (**F**) *D. phaseolorum* (DAL-222).

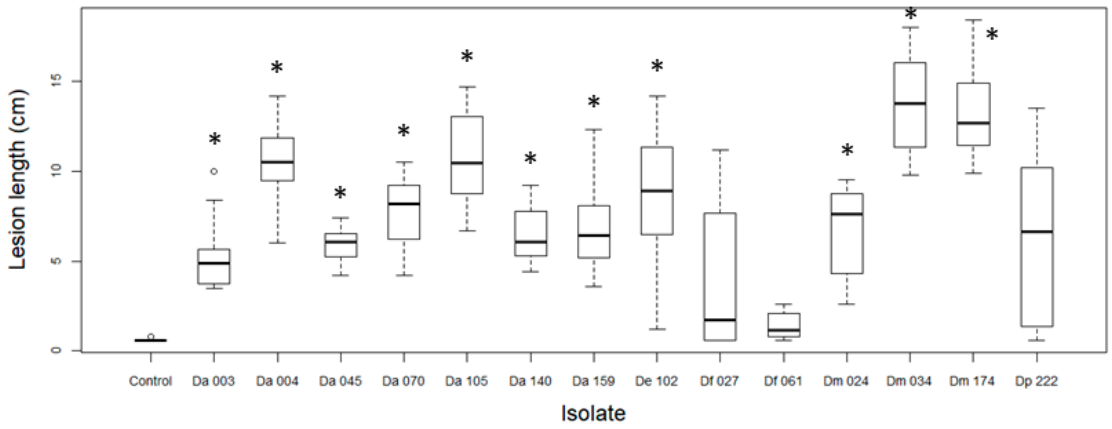

Figure 5. Box plot of lesion length (cm) caused by isolates of *Diaporthe* spp. on almond detached twigs (n = 12 per isolate) at 15 days after inoculation. Black lines in the boxes show medians. Isolate labels: Da: *D. amygdali*, De: *D. eres*, Df: *D. foeniculina*, Dp: *D. phaseolorum*, Dm: *D. mediterranea*. Asterisks (*) indicate that values are significantly different from the control according to the Wilcoxon rank sum test ($p < 0.01$).

When isolates of the different *Diaporthe* species were grouped, significant differences in mean lesion length (cm) were also observed ($p < 0.01$). Twigs inoculated with *D. mediterranea* showed significantly longer mean lesions (11.3 cm) compared with *D. amygdali*. (Figure 6). There were no statistical differences among mean lesion length values caused by *D. amygdali* (7.7 cm), *D. eres* (8.4 cm) or *D. phaseolorum* (6.2 cm). However, twigs inoculated with *D. foeniculina* showed significantly shorter lesions (2.6 cm) compared with the other *Diaporthe* spp., except for *D. phaseolorum*.

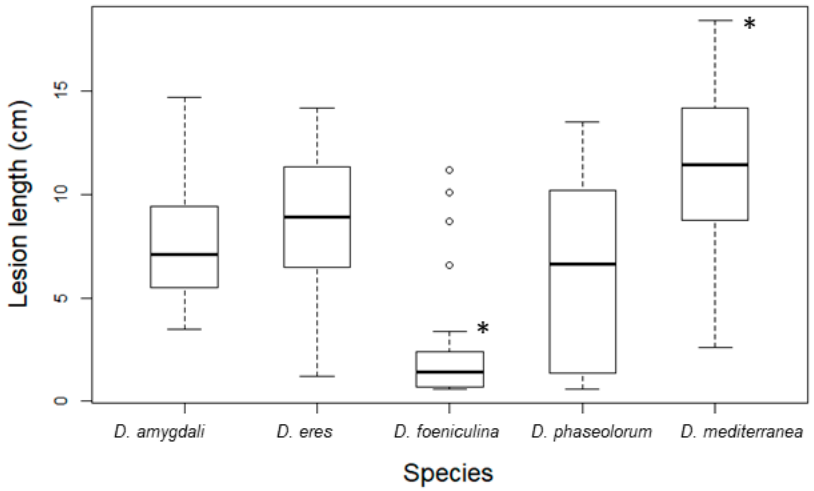

Figure 6. Box plot of lesion length (cm) caused by *Diaporthe* spp. on almond detached twigs inoculated (n = 12 per isolate) with isolates of *D. amygdali* (seven isolates), *D. eres* (one isolate), *D. foeniculina* (two isolates), *D. phaseolorum* (one isolate) and *D. mediterranea* (three isolates). Black lines in the boxes show medians. Asterisks (*) indicate that values are significantly different than *D. amygdali* according to the Wilcoxon rank sum test ($p < 0.01$).

4. Discussion

The survey conducted on almond orchards showing twig cankers and shoot blight symptoms in five different regions of Spain from 2005 to 2019 resulted in a collection of 225 *Diaporthe* isolates, which were used to elucidate the diversity of *Diaporthe* species associated with this host using both phenotypical data and DNA sequence analyses.

This is the first study in which a collection of *Diaporthe* isolates from almond has been characterized using multilocus DNA sequence analysis with five loci (ITS, *tub*, *tef-1α*, *cal* and *his*), which has been recommended in previous phylogenetic studies of the genus *Diaporthe* for species identification and separation [14,17,44]. This analysis allowed the identification of four known *Diaporthe* species, namely: *D. amygdali*, *D. eres*, *D. foeniculina* and *D. phaseolorum*. Moreover, it also confirmed that eight isolates represented a novel phylogenetic species, newly described here as *D. mediterranea*.

Diaporthe amygdali was the most prevalent species, due to the largest number of isolates collected from widely separated almond growing regions in Spain. This fungus has been described on this crop in other Mediterranean countries, such as France [11], Greece [45], Hungary [46], Italy [47], Portugal [8,48] and Tunisia [49], where it is considered the main pathogen associated with twig cankers and shoot blight symptoms. In Mediterranean areas, *D. amygdali* has also been reported as a damaging agent in other fruit and nut crops, such as apricot [50], peach [9,51] and English walnut [52]. *Diaporthe amygdali* is also present in other continents, affecting diverse hosts: on almond and peach in the USA [53,54]; grapevine in South Africa [55]; peach in Japan [56]; peach and nectarine in Uruguay [57,58]; and peach, pear and walnut in China [59–61].

Regarding the other *Diaporthe* species found in our study: *D. eres* was previously reported on *P. dulcis* in Portugal [8], and *D. foeniculina* is present on almond in Italy, with one isolate (CBS 171.78) deposited at the Westerdijk Fungal Biodiversity Institute (Utrecht, the Netherlands) [62]. To our knowledge, our study represents the first report of *D. phaseolorum* on almond.

The isolates described in our work as belonging to the new taxon, *D. mediterranea*, were found only in two almond-growing regions in Spain: coastal areas of Alicante province (Comunidad Valenciana) and Mallorca (Islas Baleares). It is interesting to note that the ITS and *tub* sequences of two *Diaporthe* isolates, namely *Phomopsis* sp. 5 (PMM 1657 and PMM 1660), which were collected from *V. vinifera* in South Africa [41,42], showed 100% identity with the ITS and *tub* sequences of *D. mediterranea*. Further studies including other loci would be needed to resolve the identity of the South African isolates (PMM 1657 and PMM 1660).

Pathogenicity tests were performed using one-year-old almond twigs, as described by [8], who determined the capacity of *Diaporthe* spp. isolates from Portugal to cause lesions on this crop. Except for *D. foeniculina* and *D. phaseolorum*, all *Diaporthe* species inoculated to almond twigs cv. Vayro were able to cause lesions significantly different from those developed on the uninoculated controls. The most severe symptoms were detected on almond twigs inoculated with *D. mediterranea*. Therefore, this study provides novel information about the ability of this species to cause disease on *P. dulcis*, being more aggressive than the well-known pathogen *D. amygdali*. *Diaporthe eres* was also pathogenic to almond, but the incidence of this species and *D. phaseolorum* in the survey conducted in this study was extremely low, with only one isolate found in each species.

The present study is the first comprehensive attempt to characterize *Diaporthe* species associated with *P. dulcis* in Spain, combining morphology and multilocus DNA sequence analysis. Our results confirm *D. amygdali* as a key pathogen of almonds in Spain. Moreover, the new species *D. mediterranea* should also be considered as a potentially important causal agent of twig cankers and shoot blight on this crop, according to the high virulence shown in the pathogenicity tests. In Spain, the lack of information regarding the identity of *Diaporthe* species on almond and their pathogenicity hinders the development of efficient control strategies and the development of resistant varieties. These aspects have been addressed for the first time in this work and will contribute to the development of improved integrated disease management programs against twig canker and shoot blight disease.

Author Contributions: Conceptualization, M.L., M.B., G.E. and J.A.; Methodology, M.L., M.B., J.M.R.-R., G.E., P.A.-C., A.R.-A. and J.A.; Software, M.L. and M.B.; Validation, M.L., M.B., J.M.R.-R. and J.A.; Formal Analysis, M.L., M.B., J.M.R.-R. and J.A.; Investigation, M.L., M.B., J.M.R.-R., G.E., P.A.-C., A.R.-A. and J.A.; Resources, D.O., A.V., J.L., X.M., C.A.-B., A.T., N.C., F.T.A., M.A., D.G. and M.A.-S.; Data Curation, M.L., J.M.R.-R. and J.A.; Writing—Original Draft Preparation, M.L., M.B. and J.A.; Writing—Review and Editing, M.L., M.B., J.M.R.-R., G.E., P.A.-C., A.R.-A., D.O., A.V., J.L., X.M., C.A.-B., A.T., N.C., F.T.A., M.A., D.G., M.A.-S. and J.A.; Visualization, M.L., M.B. and J.A. All authors have read and agreed to the published version of the manuscript.

Funding: Research funded by the Instituto Nacional de Investigación y Tecnología Agraria y Alimentaria (INIA), grants RTA2017-00009-C04-01, -02, -03 and -04 and with matching funds from the European Regional Development Fund (ERDF). G. Elena and C. Agustí-Brisach were supported by the Spanish post-doctoral grants "Juan de la Cierva-Formación" and "Juan de la Cierva-Incorporación", respectively. J. Luque and X. Miarnau were partially supported by the CERCA program, Generalitat de Catalunya. D. Gramaje was supported by the Ramón y Cajal program, Spanish Government (RYC-2017-23098).

Acknowledgments: We thank P. Yécora for her technical support.

Conflicts of Interest: The authors declare no conflict of interest.

References

1. FAOSTAT. Food and Agriculture Organization of the United Nations. 2018. Available online: http://www.fao.org/faostat/es/#dat (accessed on 1 June 2020).
2. MAPA Anuario de Estadística Agraria. 2019. Available online: https://www.mapa.gob.es/es/estadistica/ (accessed on 1 June 2020).
3. Egea, J.; Dicenta, F. Algunas consideraciones sobre el cultivo del almendro en secano. *Fruticultura* **2016**, *49*, 102–111.
4. Miarnau, X.; Torguet, L.; Batlle, I.; Alegre, S. El cultivo del almendro en alta densidad. *Fruticultura* **2016**, *49*, 68–87.
5. Barrios-Sanromà, G.; Aymamí-Besora, A. El futuro de la sanidad vegetal del almendro. *Fruticultura* **2016**, *49*, 128–151.
6. Ollero-Lara, A.; López-Moral, A.; Lovera, M.; Raya, M.C.; Roca, L.F.; Arquero, O.; Trapero, A. Las enfermedades del almendro en Andalucía. *Fruticultura* **2016**, *49*, 166–183.
7. Adaskaveg, J.E. Phomopsis canker and fruit rot. In *Compendium of Nut Crop Diseases in Temperate Zones*; Teviotdale, B.L., Michailides, T.J., Pscheidt, J.W., Eds.; APS Press: St. Paul, MN, USA, 2002; pp. 27–28.
8. Diogo, E.L.F.; Santos, J.M.; Phillips, A.J.L. Phylogeny, morphology and pathogenicity of *Diaporthe* and *Phomopsis* species on almond in Portugal. *Fungal Divers.* **2010**, *44*, 107–115. [CrossRef]
9. Tuset, J.J.; Portilla, M.T. Taxonomic status of *Fusicoccum amygdali* and *Phomopsis amygdalina*. *Can. J. Bot.* **1989**, *67*, 1275–1280. [CrossRef]
10. Tuset, J.J.; Hinarejos, C.; Portilla, M.T. Incidence of *Phomopsis amygdali*, *Botryosphaeria berengeriana* and *Valsa cincta* diseases in almond under different control strategies. *EPPO Bull.* **1997**, *27*, 449–454. [CrossRef]
11. Delacroix, G. Sur une maladie des amandiers en Provence. *Bull. Trimest. Soc. Mycol. Fr.* **1905**, *21*, 180–185.
12. Udayanga, D.; Liu, X.; Crous, P.W.; McKenzie, E.H.C.; Chukeatirote, E.; Hyde, K.D. A multi-locus phylogenetic evaluation of *Diaporthe* (*Phomopsis*). *Fungal Divers.* **2012**, *56*, 157–171. [CrossRef]
13. Rossman, A.Y.; Adams, G.C.; Cannon, P.F.; Castlebury, L.A.; Crous, P.W.; Gryzenhout, M.; Jaklitsch, W.M.; Mejía, L.C.; Stoykov, D.; Udayanga, D.; et al. Recommendations of generic names in Diaporthales competing for protection or use. *IMA Fungus* **2015**, *6*, 145–154. [CrossRef]
14. Gomes, R.R.; Glienke, C.; Videira, S.I.R.; Lombard, L.; Groenewald, J.Z.; Crous, P.W. *Diaporthe*: A genus of endophytic, saprobic and plant pathogenic fungi. *Persoonia* **2013**, *31*, 1–41. [CrossRef]
15. Gao, Y.; Lui, F.; Duan, W.; Crous, P.W.; Cai, L. *Diaporthe* is paraphyletic. *IMA Fungus* **2017**, *8*, 153–187. [CrossRef]
16. Dissanayake, A.J.; Phillips, A.J.L.; Hyde, K.D.; Yan, J.Y.; Li, X.H. The current status of species in *Diaporthe*. *Mycosphere* **2017**, *8*, 1106–1156. [CrossRef]
17. Santos, L.; Alves, A.; Alves, R. Evaluating multi-locus phylogenies for species boundaries determination in the genus *Diaporthe*. *PeerJ* **2017**, *5*, e3120. [CrossRef]
18. Lawrence, D.P.; Travadon, R.; Baumgartner, K. Diversity of *Diaporthe* species associated with wood cankers of fruit and nut crops in northern California. *Mycologia* **2015**, *107*, 926–940. [CrossRef]
19. Gramaje, D.; Agustí-Brisach, C.; Pérez-Sierra, A.; Moralejo, E.; Olmo, D.; Mostert, L.; Damm, U.; Armengol, J. Fungal trunk pathogens associated with Wood decay of almond trees on Mallorca (Spain). *Persoonia* **2012**, *28*, 1–13. [CrossRef]
20. Gardes, M.; Bruns, T.D. ITS primers with enhanced specificity for basiodiomycetes-applications to the identification of mycorrhizae and rusts. *Mol. Ecol.* **1993**, *2*, 113–118. [CrossRef]

21. White, T.J.; Bruns, T.D.; Lee, S.B.; Taylor, J.W. Amplification and direct sequencing of fungal ribosomal RNA genes for phylogenetics. In *PCR Protocols—A Guide to Methods and Applications*; Innis, M.A., Gelfand, D.H., Sninsky, J.J., White, T.J., Eds.; Academic Press: New York, NY, USA, 1990; pp. 315–322.
22. Alves, A.; Crous, P.W.; Correia, A.; Phillips, A.J.L. Morphological and molecular data reveal cryptic speciation in *Lasiodiplodia theobromae*. *Fungal Divers.* **2008**, *28*, 1–13.
23. Travadon, R.; Lawrence, D.P.; Rooney-Latham, S.; Gubler, W.D.; Wilcox, W.F.; Rolshausen, P.E.; Baumgartner, K. *Cadophora* species associated with wood-decay of grapevine in North America. *Fungal Biol.* **2015**, *119*, 53–66. [CrossRef]
24. O'Donnell, K.; Cigelnik, E. Two divergent intragenomic rDNA ITS2 types within a monophyletic lineage of the fungus *Fusarium* are nonorthologous. *Mol. Phylogenet. Evol.* **1997**, *7*, 103–116.
25. Glass, N.L.; Donaldson, G. Development of primer sets designed for use with PCR to amplify conserved genes from filamentous ascomycetes. *Appl. Environ. Microb.* **1995**, *61*, 1323–1330. [CrossRef]
26. Crous, P.W.; Groenewald, J.Z.; Risède, J.M.; Simoneau, P.; Hywel-Jones, N.L. *Calonectria* species and their *Cylindrocladium* anamorphs: Species with sphaeropedunculate vesicles. *Stud. Mycol.* **2004**, *50*, 415–430.
27. Weir, B.S.; Johnston, P.R.; Damm, U. The *Colletotrichum gloeosporioides* species complex. *Stud. Mycol.* **2012**, *73*, 115–180. [CrossRef] [PubMed]
28. Udayanga, D.; Castlebury, L.A.; Rossman, A.Y.; Hyde, K.D. Species limits in *Diaporthe*: Molecular re-assessment of *D. citri*, *D. cytosporella*, *D. foeniculina* and *D. rudis*. *Persoonia* **2014**, *32*, 83–101. [CrossRef] [PubMed]
29. Thompson, J.D.; Higgins, D.G.; Gibson, T.J. CLUSTAL W: Improving the sensitivity of progressive multiple sequence alignment through sequence weighting, position-specific gap penalties and weight matrix choice. *Nucleic Acids Res.* **1994**, *22*, 4673–4680. [CrossRef]
30. Kumar, S.; Stecher, G.; Li, M.; Knyaz, C.; Tamura, K. MEGA X: Molecular Evolutionary Genetics Analysis across computing platforms. *Mol. Biol. Evol.* **2018**, *35*, 1547–1549. [CrossRef]
31. Vaidya, G.; Lohman, D.J.; Meier, R. SequenceMatrix: Concatenation software for the fast assembly of multi-gene datasets with character set and codon information. *Cladistics* **2011**, *27*, 171–180. [CrossRef]
32. Ronquist, F.; Teslenko, M.; van der Mark, P.; Ayers, D.L.; Darling, A.; Höhna, S.; Larget, B.; Liu, L.; Suchard, M.A.; Huelsenbeck, J.P. MrBayes 3.2: Efficient Bayesian phylogenetic inference and model choice across a large modelspace. *Syst. Biol.* **2012**, *61*, 539–542. [CrossRef]
33. Miller, M.A.; Pfeiffer, W.; Schwartz, T. Creating the CIPRES Science Gateway for inference of large phylogenetic trees. In Proceedings of the Gateway Computing Environments Workshop (GCE), New Orleans, LA, USA, 14 November 2010; pp. 1–8.
34. Nylander, J.A.A. *MrModeltest v2. (Program Distributed by the Author.) Evolutionary Biology Centre*; Uppsala University: Uppsala, Sweden, 2004.
35. Stamatakis, A. RAxML version 8: A tool for phylogenetic analysis and post-analysis of large phylogenies. *Bioinformatics* **2014**, *30*, 1312–1313. [CrossRef]
36. Felsenstein, J. Confidence limits on phylogenies: An approach using the bootstrap. *Evolution* **1985**, *39*, 783–791. [CrossRef]
37. Rayner, R.W. *A Mycological Colour Chart*; Commonwealth Mycological Institute: Kew, UK, 1970.
38. Duthie, J.A. Models of the response of foliar parasites to the combined effects of temperature and duration of wetness. *Phytopathology* **1997**, *87*, 1088–1095. [CrossRef] [PubMed]
39. R Core Team. R. *A Language and Environment for Statistical Computing; R Foundation for Statistical Computing*; R Core Team. R: Vienna, Austria, 2020; Available online: https://www.R-project.org/ (accessed on 1 June 2020).
40. Mendiburu, F. Agricolae: Statistical Procedures for Agricultural Research. R Package Version 1.2-3. 2015. Available online: http://CRAN.R-project.org/package=agricolae (accessed on 1 June 2020).
41. Van Niekerk, J.M.; Groenewald, J.Z.; Farr, D.F.; Fourie, P.H.; Halleen, F.; Crous, P.W. Reassessment of *Phomopsis* species on grapevines. *Australas. Plant Path.* **2005**, *34*, 27–39. [CrossRef]
42. Lesuthu, P.; Mostert, L.; Spies, C.F.J.; Moyo, P.; Regnier, T.; Halleen, F. *Diaporthe nebulae* sp. nov. and first feport of *D. cynaroidis*, *D. novem*, and *D. serafiniae* on Grapevines in South Africa. *Plant Dis.* **2019**, *103*, 808–817. [CrossRef] [PubMed]
43. Lombard, L.; Van Leeuwen, G.C.; Guarnaccia, V.; Polizzi, G.; Van Rijswick, P.C.; Rosendahl, K.C.; Gabler, J.; Crous, P.W. *Diaporthe* species associated with *Vaccinium*, with specific reference to Europe. *Phytopathol. Mediterr.* **2014**, *53*, 287–299.

44. Guarnaccia, V.; Groenewald, J.Z.; Woodhall, J.; Armengol, J.; Cinelli, T.; Eichmeier, A.; Ezra, D.; Fontaine, F.; Gramaje, D.; Gutiérrez-Aguirregabiria, A.; et al. *Diaporthe* diversity and pathogenicity revealed from a broad survey of grapevine diseases in Europe. *Persoonia* **2018**, *40*, 135–153. [CrossRef]
45. Pantidou, M.E. *Fungus-host index for Greece*; Benaki Phytopathological Institute: Kiphissia, Athens, 1973; p. 382.
46. Varjas, V.; Vajna, L.; Izsépi, F.; Nagy, G.; Pájtli, É. First report of *Phomopsis amygdali* causing twig canker on almond in Hungary. *Plant Dis.* **2017**, *101*, 1674. [CrossRef]
47. Canonaco, A. Il seccume dei rameti di mandorlo in relazione ad alcuni micromiceti. *Riv. Patol. Veget.* **1936**, *26*, 145–164.
48. Dias, M.R.S.; Lucas, M.T.; Lopes, M.C. Fungi Lusitaniae XXIX. *Agron. Lusit.* **1982**, *41*, 175–192.
49. Trigui, A. Sur la présence en Tunisie de *Fusicoccum amygdali* Delacroix sur Amandier. *Bull. ENSAT* **1968**, *18*, 65–68.
50. Garofalo, F. L'Albicocco "Tonda di Costigliole", nuovo ospite di *Fusicoccum amygdali* Del. *Inf. Fitopatol.* **1973**, *23*, 13–15.
51. Michailides, T.J.; Thomidis, T. First Report of *Phomopsis amygdali* Causing Fruit Rot on Peaches in Greece. *Plant Dis.* **2006**, *90*, 1551. [CrossRef] [PubMed]
52. López-Moral, A.; Lovera, M.; Raya, M.C.; Cortés-Cosano, N.; Arquero, O.; Trapero, A.; Agustí-Brisach, C. Etiology of branch dieback and shoot blight of English walnut caused by Botryosphaeriaceae and *Diaporthe* Species in Southern Spain. *Plant Dis.* **2020**, *104*, 533–550. [CrossRef] [PubMed]
53. Adaskaveg, J.E.; Forster, H.; Connell, J.H. First report of fruit rot and associated branch dieback of almond in California caused by a *Phomopsis* species tentatively identified as *P. amygdali*. *Plant Dis.* **1999**, *83*, 1073. [CrossRef] [PubMed]
54. Farr, D.F.; Castlebury, L.A.; Pardo-Schultheiss, R. *Phomopsis amygdali* causes peach shoot blight of cultivated peach trees in the southeastern United States. *Mycologia* **1999**, *91*, 1008–1015. [CrossRef]
55. Mostert, L.; Crous, P.W.; Kang, J.C.; Phillips, A.J.L. Species of *Phomopsis* and a *Libertella* sp. occurring on grapevines with specific reference to South Africa: Morphological, cultural, molecular and pathological characterization. *Mycologia* **2001**, *93*, 146–167. [CrossRef]
56. Kanematsu, S.; Yokoyama, Y.; Kobayashi, T. Taxonomic reassessment of the causal fungus of peach *Fusicoccum* canker in Japan. *Ann. Phytopathol. Soc. Jpn.* **1999**, *65*, 531–536. [CrossRef]
57. Álvarez, M.I.; Perdomo, E.; Martínez, E.S.; Mondino, P.; Alaniz, S. Phomopsis amygdali principal agente causal de la viruela de la púa en durazneros y nectarinos en Uruguay. In *Abstracts of the 13th National Congress of Hortifruticulture*; INIA—Sociedad Uruguaya de Horti-Fruticultura: Montevideo, Uruguay, 2014; p. 91.
58. Sessa, L.; Abreo, E.; Bettucci, L.; Lupo, S. Diversity and virulence of *Diaporthe* species associated with wood disease symptoms in deciduous fruit trees in Uruguay. *Phytopathol. Mediterr.* **2017**, *56*, 431–444.
59. Dai, F.M.; Zeng, R.; Lu, J.P. First report of twig canker on peach caused by *Phomopsis amygdali* in China. *Plant Dis.* **2012**, *96*, 288. [CrossRef]
60. Bai, Q.; Zhai, L.; Chen, X.; Hong, N.; Xu, W.; Wang, G. Biological and molecular characterization of five *Phomopsis* species associated with pear shoot canker in China. *Plant Dis.* **2015**, *99*, 1704–1712. [CrossRef]
61. Meng, L.; Yu, C.; Wang, C.; Li, G. First report of *Diaporthe amygdali* causing walnut twig canker in Shandong province of China. *Plant Dis.* **2018**, *102*, 1859. [CrossRef]
62. Santos, L.; Phillips, A.J.L.; Crous, P.W.; Alves, A. *Diaporthe* species on Rosaceae with descriptions of *D. pyracanthae* sp. nov. and *D. malorum* sp. nov. *Mycosphere* **2017**, *8*, 485–511. [CrossRef]